Engineering and Technology Journal
Journal homepage: https://etj.uotechnology.edu.iq

Validation of the simulation implant design approach based on ct scan images and the biomechanical performance response of rehabilitated skull bones

Nareen H. Obaeed[a*], **Wisam K. Hamdan**[b]

[a] Production Engineering and Metallurgy Dept., University of Technology-Iraq, Alsina'a street, 10066 Baghdad, Iraq.
[b] Biomedical Engineering Dept., University of Technology-Iraq, Alsina'a street, 10066 Baghdad, Iraq.
*Corresponding author Email: Nareen.H.Obaeed@uotechnology.edu.iq

HIGHLIGHTS

- A high-quality, patient-specific cranial implant was designed using computed tomography (CT) images.
- Finite element analysis (FEA) was used to assess stress distribution and deformation in biomechanics.
- A biomechanical comparison of autologous skull bone and polymethylmethacrylate implants was conducted.

ARTICLE INFO

Handling editor: Israa A. Aziz

Keywords:
Cranioplasty
Polymethylmethacrylate PMMA
Finite element analysis
Cranial implant
Mechanical properties

ABSTRACT

Appropriate cranial implants are essential due to a worldwide population that is aging and the rising incidence of trauma. One key element affecting cranial implants' performance is their biomechanical behavior in human skull bones. This paper describes a high-quality cranial implant design approach for the defective skull based on computed tomography CT scan images and the biomechanical performance analysis of rehabilitation human skull bones. The valuable contribution of this work is the effective utilization of finite element analysis FEA to contrast the material behaviors of Polymethylmethacrylate PMMA cranial implants and autologous skull bone during rehabilitation as exposed to external trauma. The external loads applied in the implant's center are attached to a damaged cranium (300, 600, and 1000 N). The findings indicated that the equivalent stresses of PMMA are close to the skull bone. Minimum and maximum Von Mises stresses are (13 and 47 MPa) when employing a PMMA implant material and (12 and 41 MPa) when utilizing autologous skull bone at the lowest and highest level of applied force (300 and 1000 N), respectively. In terms of deformation distribution (0.02 and 0.03 mm) at applying 300 N, approximately six times the weight of a human head when the reconstruction is performed by skull bone and PMMA, respectively. So, this study will offer an insightful look at the neurocranial protection of PMMA implants that provide the coupling of skull bone-PMMA cranial implant, which guarantees adequate protection for the internal structures of the restored area similar to the autologous skull bone.

1. Introduction

The human skull bone is a heterogeneous biomaterial that plays a vital role in human life safety. Head trauma is frequently caused by the impact of foreign objects in accidents, warfare shrapnel, or building collapses [1]. Suppose the patient's bone cannot be used to rebuild the overall integrity of the patient's skull. In that case, the lost portion must be replaced with thermoplastic, resin plates, or metal components having mechanical characteristics resembling those of human bone [2]. Cranial bone is a complicated material with three layers: the outermost layers are compact, high-density cortical bone, and the core layer is a low-density, irregularly porous structure of bone [3,4]. Cranial implants have witnessed significant and remarkable development during the last decade due to the massive population explosion and the high rates of external trauma, in addition to congenital cranial defects [5]. Cranioplasty is the surgical process of correcting cranial abnormalities by carefully replacing the missing bone [6-9]. Continuous advancements in cranioplasty procedures have enabled the correction of massive and increasingly complex calvarial abnormalities.The gold standard for cranioplasty is autologous bone; however, a synthetic cranial implant is employed when autologous bone is not an option due to fracture, infection, etc. Nevertheless, the best reconstructive material for many clinical circumstances remains unknown and debated [10]. Currently, titanium alloy

http://doi.org/10.30684/etj.2024.148915.1735
Received 17 April 2024; Received in revised form 23 May 2024; Accepted 24 May 2024; Available online 10 July 2024
2412-0758/University of Technology-Iraq, Baghdad, Iraq

Ti6Al4V, Polymethylmethacrylate (PMMA), and Polyetheretherketone (PEEK) are the most often utilized biomaterials for cranial implants [11,12]. PEEK and PMMA share several characteristics overall. Both preserve biomechanical characteristics comparable to bone while being readily moldable and biologically inert [13]. PMMA is a thermoplastic that is commonly known as "organic glass." PMMA exhibits several remarkable properties, including low shrinkage, excellent weather resistance, high elastic modulus, biocompatibility, lightweight, and elevated hardness [14].The size and location of the defect typically determine the implant thickness, and the required functional stiffness can also be determined [15]. Perfect material for a cranioplasty should be flexible and radiolucent; it is not heat or cold conductive, biocompatible, inert, non-infectious, well-fitting, low-cost, and capable of encouraging tissue growth [16,17]. Several crucial requirements must be addressed when choosing cranial implants, including biocompatibility, specialized geometry to guarantee close integration with bone tissue, and sufficient mechanical characteristics to tolerate function-related stress [18].The FEA model has been employed to evaluate the biomechanical reliability of the specific cranial implant constructed [19]. A proper simulation study can help determine the mechanical parameters that the medical devices provided to patients must have to be capable of supporting certain static loads or simulating some occurrences that may happen throughout the performance of tasks.

The models generated by cranial implants have been validated using various techniques, software, and methodologies. Chamrad et al. [20] based on a PMMA skull implant, evaluate the precision of the bone-implant interface. Computational simulation was used to conduct the evaluation. Ameen et al. [21] utilized finite element analysis to design and assess a custom cranial implant before using electron beam melting (EBM) additive manufacturing to create the implant from titanium alloy Ti6Al4V. The proposed design's functionality, appropriateness, and aesthetics are assessed. The outcomes show that a thin cranial implant created using EBM technology was successfully fabricated. Wu et al. [1] systematically examine the failure process of cranium cellular bones and their capacity to absorb energy under low and medium-velocity loadings.

The effects of several typical characteristics, including the impact speed, impact angle, impactor geometry and density, and different restored sections, on the impact performance of human skull biological bones are examined. Santos et al. [22] designed a cranial implant to fill a deficiency in the skull and then investigated its mechanical efficiency by integrating it into the human skull's finite element model. The implant was made of PEEK, which was analyzed to determine two factors: the number of fixing screws and the implant's ability to preserve the brain when compared to the integrated skull. Moncayo-Matute et al. [23] comparative analysis using finite elements is used to simulate the mechanical reaction of a medical device with two different materials: Polymethylmethacrylate and Polyetheretherketone are materials of choice for engineering applications owing to their superior mechanical properties. The results thus demonstrated how closely their responses aligned to each material. Kim et al. [12] simulated the asymmetric defect skull model using the finite element method during intracranial pressures and a fixed load of 50 N imposed at three sites for PEEK cranial implant. Rodríguez et al. [24] studied the relation between thickness and stiffness for PMMA and PEEK materials used in patient-specific cranial implants. Displacement distributions under critical loading circumstances are determined from the finite element analysis by incorporating design aspects like thickness and perforations. To avoid severe deformations over 2 mm, both biomaterials exhibit the lowest mechanical parameter to withstand direct trauma. Previous research often focuses on synthetic materials such as cranial implants. Most studies focused on applying a force of 50 N, which is equivalent to the weight of an adult human head. This investigation is based on reconstructing the defective skull by designing high-quality patient-specific cranial implants based on CT scan images. It compares the biomechanical responses of reconstructed defective skull bone using identical autologous skull bone implants and PMMA implants when exposed to external trauma (300, 600, and 1000 N). So, a new vision is to compare the reconstruction by a skull bone-autologous skull bone implant and a skull bone-PMMA implant of a defective skull that has been rehabilitated.

2. Design of patient-specific implant

2.1 Data acquisition and image processing

The patient's computed tomography scan data has been obtained as a Digital Imaging and Communications in Medicine (DICOM) file from the Neurosurgery Teaching Hospital in Baghdad, Iraq. Figure 1 illustrates the CT scan device and the two-dimensional 2D image has been produced from this device.

(a) **(b)**

Figure 1: (a): CT scan device, (b): Images generated from the device

A computed tomography scan combines several X-ray images of the patient's skull from various angles to produce cross-sectional images (slices) of the bones, conducted with the skull's axial, sagittal, and coronal planed with a 512 × 512 pixels matrix. The design engineers have access to the DICOM file format, which comprises a collection of two-dimensional (2D) images stored in a database that can be accessed. A 3D digital image of the skull is generated utilizing a specific medical modeling software called Mimics 21.0 (Materialise, Leuven, Belgium) to process the DICOM images. CT 2D slice pictures are segmented by selecting specific image intensities inside the region of interest. Density-based thresholding using Hounsfield units was utilized to reduce image noise and prevent softer materials such as skin, brain, and so on from appearing in the visualization. The hard and soft tissues are distinguished using a grayscale Hounsfield units (HU) measurement. Materials like air, tissue, bone, etc., have varying capacities to absorb radiation. HU refers to the coefficient of radiation (X-ray and CT) absorption. To divide the region of interest, the segmentation approach based on thresholding was used to eliminate foreign data where a Boolean value denotes 0 of an empty space or no material, and 1 denotes the skull's material; Figure 2 illustrates this transition.

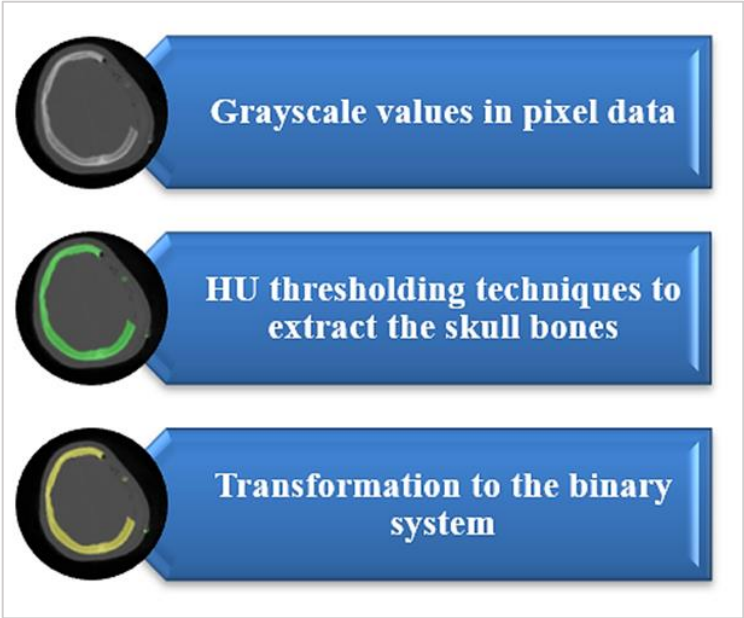

Figure 2: Converting the image to binary format

To further process, build, and finally construct the patient-specific implant 3D model created in MIMICS 21 software was stored in the Standard Tessellation Language (.STL) data file format and exported to the 3-Matic Medical 13 (Materialise, Leuven, Belgium). Figure 3 depicts a screenshot of the MIMICS 21 program featuring scans for viewing the reconstructed 3D image skull. The three-dimensional defective skull that was created has different thicknesses at each point. Since the constructed cranium is based on actual data represented by CT scan images, these variations in thickness ranging from less than 1mm to approximately 10 mm are present throughout the color mapping model and can be visualized in Figure 4. Thus, there is a challenge in rehabilitating the defect through a designed cranial implant with a huge number of surfaces and a very complex geometry.

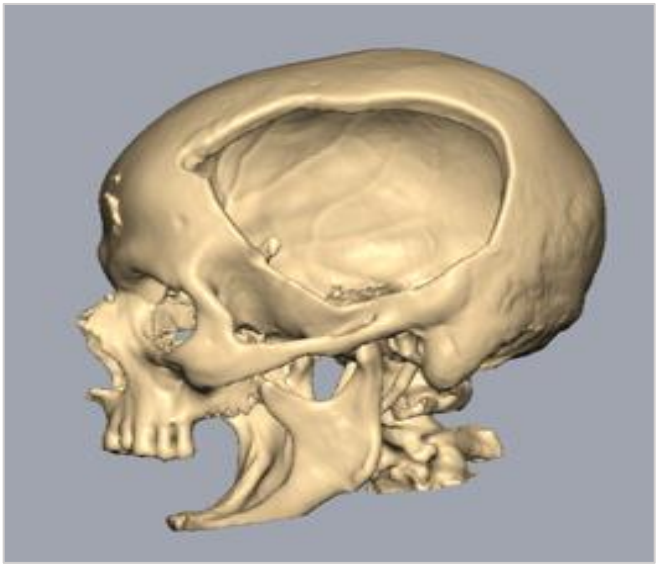

Figure 3: Three-dimensional volumetric of the defective customized skull based on CT scan images

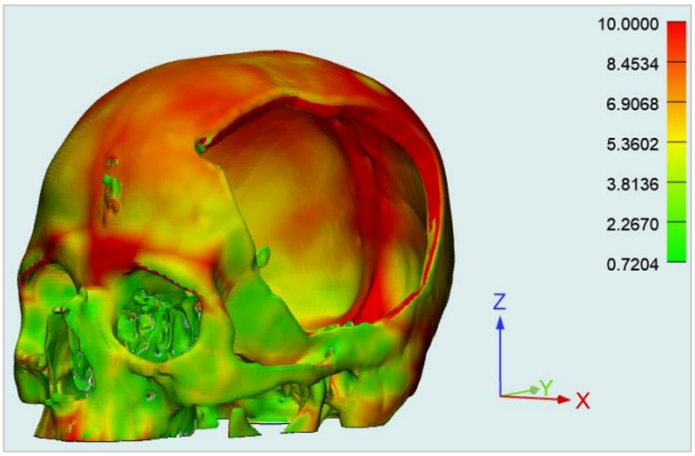

Figure 4: Thickness color mapping of customized defected skull

2.2 Cranial implant design

The reconstruction of the skull defects and the suitable cranial implant design is challenging. The alternative anatomical design technique and the mirror reconstruction technique are two well-known reconstructive approaches for implant design. In the development of cranial implants, the mirror methodology is the most often used reconstructing method technique in cranial implants [25,26]. The implant contour profile was created by projecting the flawed bone tissue's edge curvature onto the mirrored dataset, providing a flawless match of the implant borders to the defective bone tissue.

Establishing a datum plane, or as called symmetry plane, is one of the procedures involved in implant reconstruction. The healthy skull bone on the right side is inverted, resulting in a mirror image superimposed on the defective bone on the left side (trauma bone). Subsequently, the symmetrical human skull and the rebuilt skull containing defects were combined. Boolean operations subtract The combined replica skull from the reconstructed skull containing the defect, following the reconstruction of the defective skull surface. The recently formed surface was detached from the skull cavity and produced a patient-specific cranial implant, as shown in Figure 5. The designed cranial implant enables flawless continuity between the surrounding defect area and the designed implant, offering aesthetic restoration and sufficient protection.

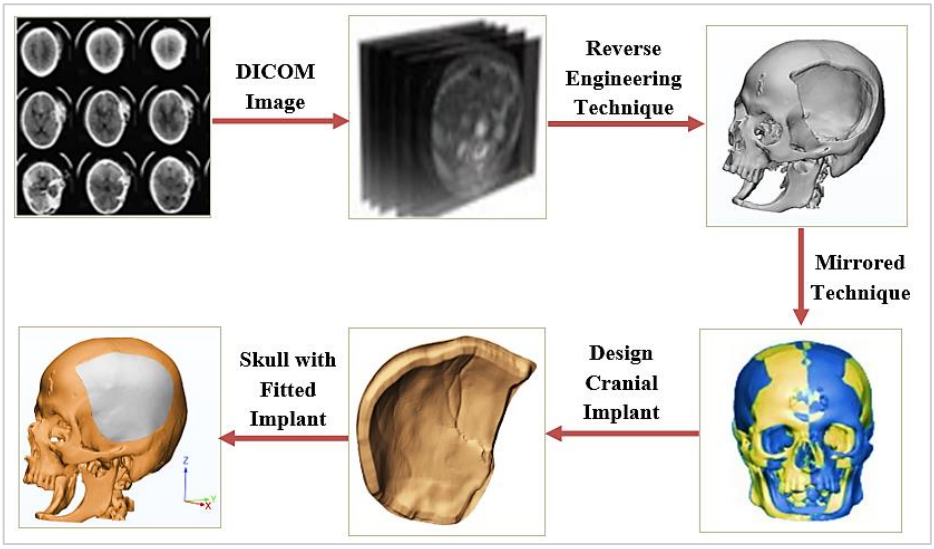

Figure 5: Summarized the primary technique to design the patient-specific cranial implant

3. Finite element analysis

A computational method for simulating the biomechanical behavior of complex structures under varied loading scenarios is finite element analysis [27]. It was employed to assess how well a specially made cranial implant worked. It allows for calculating stress, strain, and deformation by dividing the structure into discrete elements connected at nodes. FEA helps with design optimization by predicting how a structure will react to mechanical forces by applying boundary conditions and material attributes. The models were preprocessed, solved, and postprocessed using ansys workbench R1 2022 software.

The curvature of the skull's profile and the implant's position must be as accurate as possible to achieve successful implant fixation. This deals with examining the extent of the damage's perimeter and the modes of stress transfer under various external loads. Check if the interior of the cranial implant has a specific engraving that complements the edges of the skull defect. However, the best fit that can be achieved will also increase the coupling safety. Computer-aided design CAD models of the defective skull bone and designed cranial implant have meshed with continuous tetrahedral elements. High-quality meshing elements were accomplished on the skull and customized cranial implant models. A mesh sensitivity study was

conducted before selecting a mesh element size for the two models to ensure that the chosen element size was not time-consuming and was not prone to discretization errors. A total number of nodes (885047) and (586374) elements have been generated for the cranial implant and skull bone portion because of the small mesh proposed to prevent mesh distortion and increase element quality, as depicted in Figure 6. According to advice from specialist physicians, the applied static loading replicated a comfortable individual lying on a pillow [21]. Different static force values have been applied in the center of the designed cranial implant. Values of external force (300, 600, and 1000 N) were applied. The human cortical skull bone and PMMA properties have been assumed to be homogenous, isotropic, and linearly elastic. As a result, the recommended design has a high safety factor, neglecting the contact between the constructed cranial implant and the boundary skull bone. Table 1 presents the properties of the autologous cortical skull bone and PMMA characteristics [28-31] that should be considered in this study.

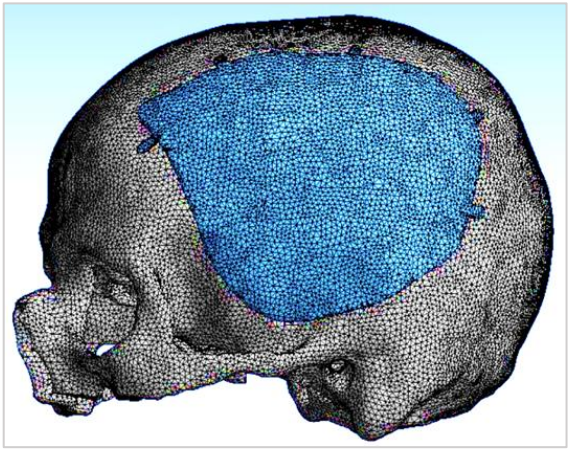

Figure 6: Mesh generation of patient-specific skull

Table 1: Material properties for the structural finite element analysis

Material	Young Modulus (Mpa)	Yield Strength (MPa)	Poisson Ratio
Autologous skull bone	13700	122	0.3
PMMA	3100	72	0.375

4. Results and discussion

The simulations were developed to evaluate the effects of varying loading according to three static external loads in coupling the defective human skull bone- patient-specific cranial implant system frameworks with two differing reconstruction materials. Deformation and equivalent stress or Von Mises stress distributions display the results obtained. Figure 7 illustrates the results of the Von Mises stress distribution of reconstruction with cortical skull bone and PMMA material as an implant, achieved by complying with the simulation FEA model execution. Figure 7 (a and b) display the equivalent stress results when applying an external force of 300 N on the center of the implant when autologous bone and synthetic PMMA material respectively. Figure 7 (c and d) display outcomes of applying 600 N on the center of the implant when autologous bone and synthetic PMMA material respectively. Figure 7 (e and f) depicts the equivalent stress at applying 1000 N of autologous bone and synthetic PMMA material respectively.

The Von Mises stress values at 300 N external load were (12.18 and 13.57 MPa) when employing autologous skull bone and a PMMA implant material, respectively. It was observed that there is a very tiny difference of approximately 1.5 MPa between the two measurements. Table 2 depicts the maximum deformation and equivalent stress values under three impact loads (300, 600, and 1000) MPa of skull bone and Polymethylmethacrylate thermoplastic material. Conversely, it has been noticed an increase in the differential of the equivalent stress to approximately 4 MPa results from (24.375 and 28.434 MPa) from the two materials of the skull bone and PMMA compensating for an external force 600N twice the applied force in the first case. The difference in Von Mises stress between these two materials increases with further exposure to force 1000 N. Mian et al. [29] showed that von Mises stress within the PEEK implant peaked at 8.15 MPa when applied a static load of 50 N, which represents one-sixth of the least force exerted in this study 300N that reflected 13.5 MPa for PMMA cranial implant. Moncayo-Matute et al. [32] showed that the Von Mises of PMMA cranial implant was 4.23 MPa when a force of 50 N was applied. These findings propose that the reconstruction of the defective skull with PMMA cranial implant is functionally satisfactory.

Figure 8 shows a comparative bar chart view of the maximum Von Mises stress between two types of material utilized in this study. As far as is known, autologous skull bone has a complex composition and microstructure of the natural bone. Its heterogeneous and anisotropic characteristics enable effective stress dispersion and dissipation. Conversely, although PMMA is well-known for its stiffness and strength, it lacks the intricacy and flexibility of natural bone. The mechanical behavior of PMMA and autologous bone differs under increasing force, which causes the PMMA implant to experience more significant

stress concentrations. The hierarchical nature of autologous skull bone facilitates the load transfer throughout the cranial vault. The bone's ability to disperse the load across a greater region in response to an external force lowers stress concentrations. In addition, due to its homogenous nature, PMMA may transmit applied force less effectively, which could result in localized stress concentrations at the force application location.

On the other hand, when mechanical stimulation is applied, natural bone can rebuild and change structurally. Besides preserving structural integrity, this adaptive response helps to reduce stress concentrations. While PMMA is an inert material, it cannot adjust to changes in force. As a result, its stress distribution stays relatively constant, leading to more significant stress concentrations. The structural integrity of autologous skull bone and PMMA exhibit significant disparities as impact force increases. To release stress, autologous bone may undergo regulated remodeling and distortion.

Despite these reasons and the slight difference between the Von Mises stress values of these two materials, the cranioplasty by polymethylmethacrylate material is considered an excellent option. It is observed that when the maximum force is applied to the human skull, the equivalent stresses obtained are one and a half times lower than the Polymethylmethacrylate's yield strength (72 MPa) see Table 1. Consequently, the PMMA implant is guaranteed to be unaffected by any plastic deformation. As a result, the recommended designs have a high safety factor.

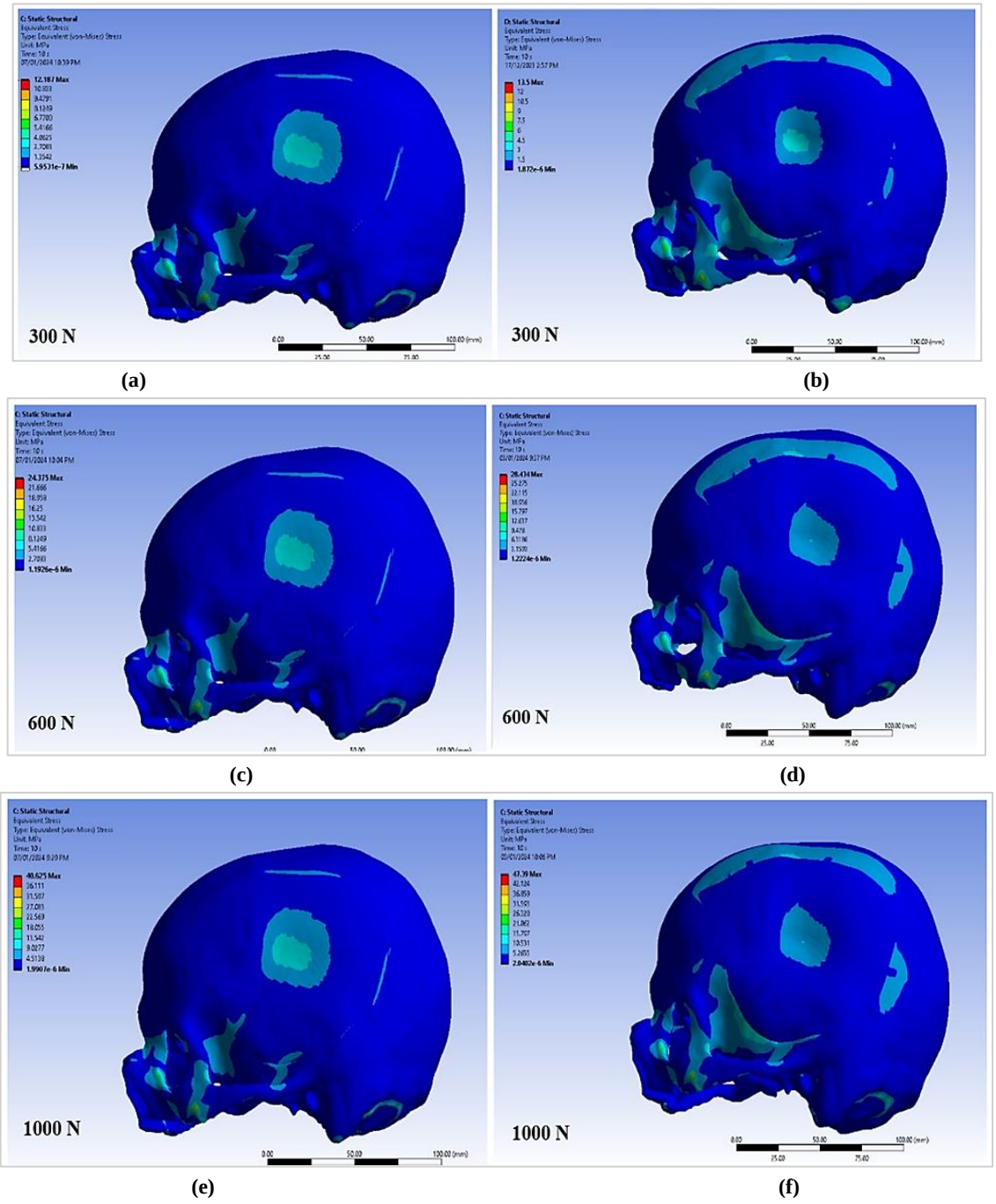

Figure 7: Equivalent (Von Mises) stress results when rehabilitating the defect by autologous skull bone (left side) and by PMMA material (right side); (a) applied 300 N on autologous skull bone, (b) applied 300 N on PMMA, (c) applied 600 N on autologous skull bone, (d) applied 600 N on PMMA, (e) applied 1000 N on PMMA, (c) applied 1000 N on autologous skull bone, (d) applied 300 N on PMMA

Table 2: Maximum deformation and equivalent stress values under different impact loads

	Cranial Material Type	Applied Load (N)	Maximum Deformation (mm)	Maximum Von Mises Stress (MPa)
1	Bone Skull Implant	300	0.0203	12.187
2		600	0.0339	24.375
3		1000	0.0613	40.625
1	PMMA Cranial Implant	300	0.0306	13.5
2		600	0.0475	28.434
3		1000	0.1022	47.39

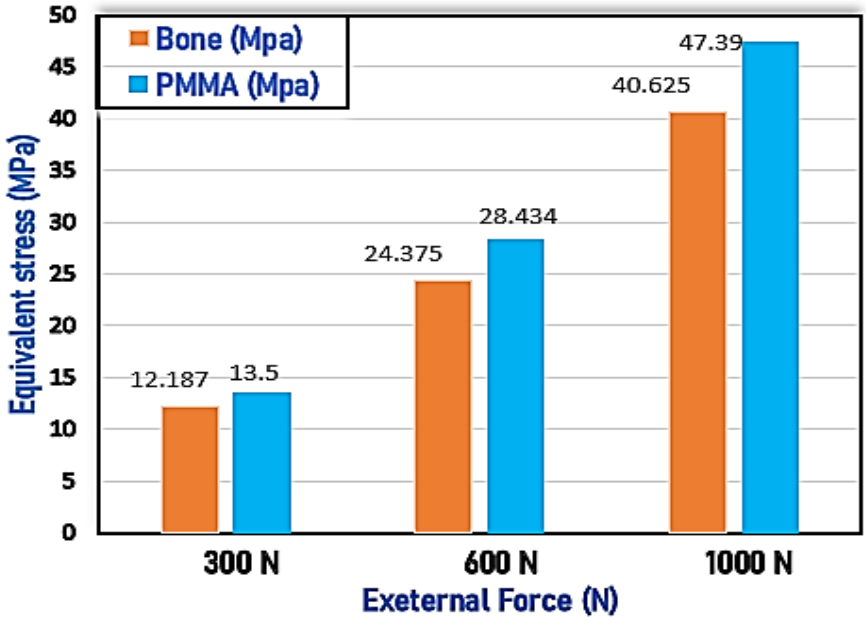

Figure 8: Comparative Von Mises chart of autologous skull bone and PMMA materials

The results of comparative finite element analysis deformation in two proposed materials considered in this study can be depicted in Figures 9 and 10. Due to the stress concentration imposed by the externally applied force, deformation is more noticeable at the center of the cranial implant. The maximum deformation related to the autologous skull implant was 0.0613 mm. PMMA was 0.1022 mm, both within the limits of elasticity values and very close compared to the large value of the applied force (1000 N). Figure 9 shows that the deformities do not occur in the exact locations or have the same orientation, whether autogenous skull bone or polymethylmethacrylate material is used for reconstructing the defect due to the difference between Young's modulus and Poisson ratio. The distribution area of deformation or displacement is more expansive when the autologous bone implant is utilized and is not concentrated in narrow areas because it is the same material surrounding the defect. In addition, the modulus of elasticity of cortical skull bone is higher (13700 MPa) than the PMMA (3100 MPa), as illustrated in Table 1. Related to the contrast of the color map evident in Figure 10, when the cranial implant is made of the same material as the defective skull, the variation in displacement is represented by a color map extended over a large area. Differences in material properties and stress distribution cause this. Whereas if the implant is a synthetic material of Polymethylmethacrylate, the color map of deformation will concentrate only around the site of the external force that is applied because:

1) The mechanical properties of the autologous cranial implant, such as density, elasticity, and strength, are probably equivalent when the two components are made of the same material. A more comprehensive range of color variation can be achieved because of more consistent stress distribution and displacement throughout the implant.
2) Since PMMA is a synthetic material, its mechanical properties typically remain consistent throughout. Because of the homogeneity of the material, stress tends to concentrate in the area where the force is applied. Consequently, color concentration happens at the close region where force application occurs since displacement or deformation focuses primarily on that location.
3) The interface between the implant and the surrounding defective skull can impact displacement distribution. Regarding displacement transmission and variation, the autologous skull bone might blend in with the surrounding section of the defective skull more naturally than using PMMA cranial implants.

Despite this distribution variation, the difference in the deformation between the two types of material used is very slight and does not exceed (0.04 mm) for the maximum applied force. So, the results obtained are close, and the deformations take a concave geometric shape, which makes using Polymethylmethacrylate provide essential protection for neurocranial tissue. The results demonstrated that the design of the implant could be utilized to rehabilitate the degenerated skull region in a manner that would prove satisfactory.

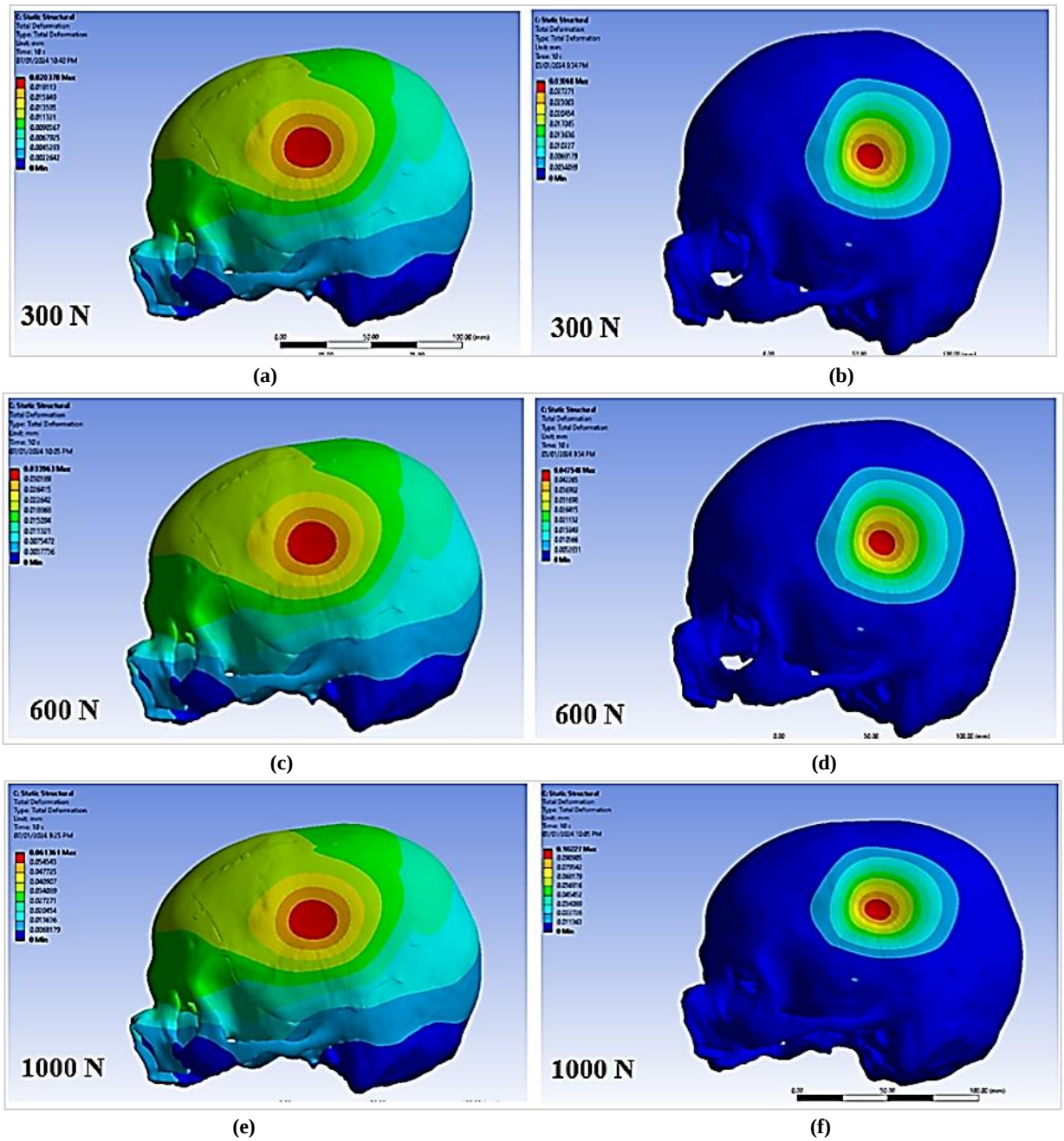

Figure 9: Deformation results that occur when rebuilt by autologous skull bone (left side) and rehabilitated by PMMA material (right side); (a) applied 300 N on autologous skull bone, (b) applied 300 N on PMMA material, (c) applied 600 N on autologous skull bone, (d) applied 600 N on PMMA material, (e) applied 1000 N on autologous skull bone, and (f) applied 1000 N on PMMA material.

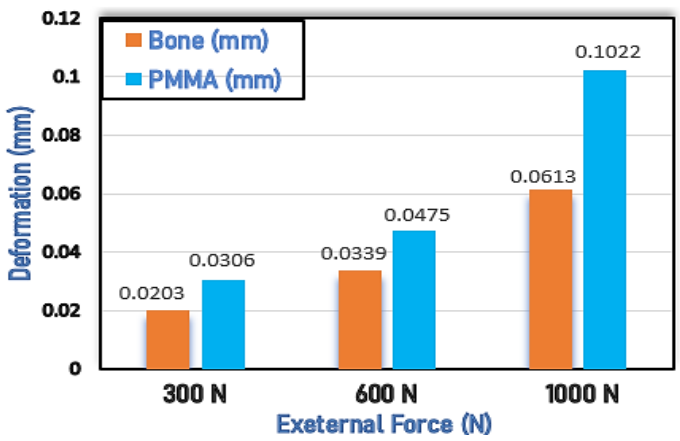

Figure 10: Comparative deformation chart of autologous skull bone and PMMA materiall

5. Conclusion

Finite element analysis is an essential step in evaluating the performance of the personalized cranial implant. It contributes to ensuring that the implant works effectively and safely after it is implanted in a patient by simulating the mechanical conditions. A cranial implant design and comparative analysis between autologous skull bone and PMMA patient-specific cranial implant of biomechanical assessment for defective skull are suggested in this work. A sophisticated understanding of the biomechanical performance of materials was used to rehabilitate skull abnormalities by conducting a dual examination of PMMA and autologous bone-mimicking materials under traumatic settings. This work represents a groundbreaking contribution to the personalized medicine of cranial implant designs since it combines rigorous FEA with CT-based patient-specific modeling. The patient-specific cranial implant was designed according to the mirror technique using MIMICS and 3-MATIC (Materialise, Leuven, Belgium). A finite element analysis was used to evaluate the quality of the developed implant design under three impact force conditions by utilizing ANSYS 2022 R1 software. The biomechanical behavior of the two cranial implant materials for a reconstructed defective skull is investigated based on stability by computing equivalent stress and deformation or displacement analysis. The minimum and maximum Von Mises stress of PMMA cranial implant has been (13.5 and 47.39 MPa) when applied external impact force (300 and 1000 N), respectively. That indicates close to the minimum and maximum results (12.187 and 40.625 MPa) when employing autologous skull bone as cranioplasty material in the same condition of applied loads. The two types of material employed exhibit tiny differences in deformation, with the highest applied force not exceeding (40 µm). Thus, the results of this study improve comprehension of rehabilitating and indicate insignificant differences between the autologous patient-specific cranial implant and the PMMA one. The future approach will aim to establish the outcome of osteointegration at various levels to predict the long-term mechanical effect of implant surfaces on bone cells.

Abbreviations

CT: Computed tomography; FEA: Finite element analysis; PMMA: Polymethylmethacrylate; PEEK: Polyetheretherketone; EBM: Electron beam melting; DICOM: Digital imaging and communications in medicine; STL: Standard tessellation language; CAD: Computer-aided design.

Author contributions

Conceptualization, N. Obaeed and W. Hamdan; data curation, N. Obaeed; formal analysis, N. Obaeed; investigation, N. Obaeed and W. Hamdan; methodology, N. Obaeed; project administration, N. Obaeed, resources, N. Obaeed; software, N. Obaeed; supervision, N. Obaeed; validation, N. Obaeed and W. Hamdan; visualization, N. Obaeed; writing—original draft preparation, N. Obaeed; writing—review and editing, N. Obaeed and W. Hamdan. All authors have read and agreed to the published version of the manuscript.

Funding

This research received no specific grant from any funding agency in the public, commercial, or not-for-profit sectors.

Data availability statement

The data that support the findings of this study are available on request from the corresponding author.

Conflicts of interest

The authors declare that there is no conflict of interest.

References

[1] Q. Wu, L. Ma , Q. Liu, L. Feng, Z. Wang, A. Ohrndorf, H. Christ, J. Xiong, Impact response and energy absorption of human skull cellular bones, J. Mech. Behav. Biomed. Mater., 81(2018)106–119. https://doi.org/10.1016/j.jmbbm.2018.02.018

[2] M. Popp, G. Rusu, S. Gabriel Racz, I. Popp, Force and thickness prediction with FEA of the cranial implants manufactured through SPIF, MATEC Web Conf., 290 (2019) 4–11. https://doi.org/10.1051/matecconf/201929004008

[3] J. Motherway, P. Verschueren, G. Perre, J. Sloten, M. Gilchrist, The mechanical properties of cranial bone: The effect of loading rate and cranial sampling position, J. Biomech., 42 (2009) 2129–2135. https://doi.org/10.1016/j.jbiomech.2009.05.030

[4] P. K. Vallittu, K. M. J. Aitasalo, A. A. Mäkitie, P. Helén, C. Lindqvist, Reconstruction of cranial bone defects with fiber-reinforced composite–bioactive glass implants, (2015).

[5] V. Bogu, Y. Kumar, A. Khanra, Homogenous scaffold-based cranial/skull implant modelling and structural analysis—unit cell algorithm-meshless approach, Med. Biol. Eng. Comput., 55 (2017) 2053–2065. https://doi.org/10.1007/s11517-017-1649-3

[6] M. Elshirbiny, A. Ahmed, M. Amen, Autograft cranioplasty for skull defects in children, Interdiscip. Neurosurg., 33 (2023) 101789. https://doi.org/10.1016/j.inat.2023.101789

[7] B. Basu, N. Bhaskar , S. Barui, V. Sharma , S. Das , N. Govindarajan, P. Hegde , P. Perikal , M. Shivakumar , K. Khanapure A. Jagannatha., Evaluation of implant properties, safety profile and clinical efficacy of patient-specific acrylic prosthesis in cranioplasty using 3D binderjet printed cranium model: A pilot study, J. Clin. Neurosci., 85 (2021) 132–142. https://doi.org/10.1016/j.jocn.2020.12.020

[8] K. Moiduddin, S. Mian, H. Alkhalefah, S. Ramalingam, A. Sayeed, Customized Cost-Effective Cranioplasty for Large Asymmetrical Defects, Processes, 11(2023)1760. https://doi.org/10.3390/pr11061760

[9] W. Abd El-Ghani, Cranioplasty with polymethyl methacrylate implant: solutions of pitfalls, Egypt. J. Neurosurg., 33 (2018) 1-4. https://doi.org/10.1186/s41984-018-0002-y

[10] H. Sable, M. Patel, K. Shah, A Prospective Comparative Study of Different Methods of Cranioplasty: Our Institutional Experience, Indian J. Neurosurg., 09 (2020) 17–23. https://doi.org/10.1055/s-0039-3402929

[11] J. Kwarcinski, P. Boughton, A. Ruys, A. Doolan, J. Gelder, Cranioplasty and craniofacial reconstruction: A review of implant material, manufacturing method and infection risk, Appl. Sci., 7 (2017) 276. https://doi.org/10.3390/app7030276

[12] C.N.T. Kim, C.X. Binh, V.T. Dung, T.V. Toan, Design and mechanical evaluation of a large cranial implant and fixation parts, Interdiscip. Neurosurg., 31 (2023) 101676. https://doi.org/10.1016/j.inat.2022.101676

[13] G. Huang, S. Zhong, S. Susarla, E. Swanson, J. Huang, C. Gordon, Craniofacial Reconstruction With Poly (Methyl Methacrylate) Customized Cranial Implants, J. Craniofac. Surg., 26 (2015) 64–70. https://doi.org/10.1097/SCS.0000000000001315

[14] N. Obaeed, W. Hamdan, Optimizing Fused Deposition Modelling Process Parameters for Medical Grade Polymethylmethacrylate Flexural Strength, Adv. Sci. Technol. Res. J., 18 (2024) 349–359. https://doi.org/10.12913/22998624/182876

[15] B. Khader, M. Towler, Materials and techniques used in cranioplasty fixation: A review, Mater. Sci. Eng. C, 66 (2016) 315–322. https://doi.org/10.1016/j.msec.2016.04.101

[16] J. Jegadeesan, M. Baldia, B. Basu, Next-generation personalized cranioplasty treatment, Acta Biomater., 154 (2022) 63–82. https://doi.org/10.1016/j.actbio.2022.10.030

[17] A. Shah, H. Jung, S. Skirboll, Materials used in cranioplasty: A history and analysis, J. Neurosurg., 36 (2014) 1–7. https://doi.org/10.3171/2014.2.FOCUS13561

[18] M. I. Martmez-Valencia, C. H. Navarro, J. A. Vazquez-Lopez, J. L. Hernandez-Arellano, J. A. Jimenez-Garda, and J. L. Dfaz-Leon, Optimization of titanium cranial implant designs using generalized reduced gradient method, analysis of finite elements, and artificial neural networks, Rev. Int. Metod. Numer. para Calc. y Disen. enIng., 38 (2022) 1-16. https://doi.org/10.23967/j.rimni.2022.06.004

[19] K. Moiduddin, S. Mian, U. Umer, H. Alkhalefah, Fabrication and analysis of a Ti6Al4V implant for cranial restoration, Appl. Sci., 9 (2019) 2513 . https://doi.org/10.3390/app9122513

[20] J. Chamrad L. Borak, Finite Element Analysis Of Cranial Implant, 22nd International Conference Engineering Mechanics, October, 2016.

[21] W. Ameen, A. Al-Ahmari, M. Mohammed, O. Abdulhameed, U. Umer, K. Moiduddin, Design, finite element analysis (FEA), and fabrication of custom titanium alloy cranial implant using electron beam melting additive manufacturing, Adv. Prod. Eng. Manag., 13 (2018) 267–278. https://doi.org/10.14743/apem2018.3.289

[22] P. Santos, G. Carmo, R. Alves, F. Fernandes, M. Ptak, Mechanical Strength Study of a Cranial Implant Using Computational Tools, Appl. Sci., 12 (2022) 878. https://doi.org/10.3390/app12020878

[23] F. Moncayo-Matute, E. Vázquez-Silva, P. Peña-Tapia, P. Torres-Jara, D. Moya-Loaiza, T. Viloria-Ávila, Finite Element Analysis of Patient-Specific 3D-Printed Cranial Implant Manufactured with PMMA and PEEK: A Mechanical Comparative Study, Polymers, 15 (2023) 3620. https://doi.org/10.3390/polym15173620

[24] M. Mejía Rodríguez, O. González-Estrada, D. Villegas-Bermúdez, Finite Element Analysis of Patient-Specific Cranial Implants under Different Design Parameters for Material Selection, Designs, 8 (2024)1-13 . https://doi.org/10.3390/designs8020031

[25] J. Egger, M. Gall, A. Tax, M. Ücal, X. Li, G. Campe, U. Schäfer, D. Schmalstieg, X. Chen., Interactive reconstructions of cranial 3D implants under MeVisLab as an alternative to commercial planning software, PLoS One, 12 (2017)1-20 . https://doi.org/10.1371/journal.pone.0172694

[26] M. Arango-Ospina C. Cortés-Rodriguez, Engineering Design and Manufacturing of Custom Craniofacial Implants, The 15th International Conference on Biomedical Engineering, 43, 2014, 908–911. https://doi.org/10.1007/978-3-319-02913-9_234

[27] N. Obaeed, Numerical and Experimental Explorations for the Formability of Drawing Square Cups Through Deep Drawing Operation , Eng. Technol. J., 38 (2020) 1316–1326. https://doi.org/10.30684/etj.v38i9A.1340/4.0

[28] A. Al-Ahmari, E. Nasr, K. Moiduddin, S. Anwar, M. Al Kindi, A. Kamrani, A comparative study on the customized design of mandibular reconstruction plates using finite element method, Adv. Mech. Eng., 7 (2015) 1–11. https://doi.org/10.1177/1687814015593890

[29] S. Mian, K. Moiduddin, S. Elseufy, H. Alkhalefah, Adaptive Mechanism for Designing a Personalized Cranial Implant and its 3d printing using peek, Polymers , 14 (2022) 1266 . https://doi.org/10.3390/polym14061266

[30] N. Sukindar, N. Samsudin, S. Shaharuddin, S. Kamaruddin, The Effects of FDM Printing Parameters on the Compression Properties of Polymethylmethacrylate (PMMA) using Finite Element Analysis, Int. J. Integr. Eng., 14 (2022) 86–92. https://doi.org/10.30880/ijie.2022.14.02.013

[31] F. Moncayo-Matute, P. Peña-Tapia, E. Vázquez-Silva, P. Torres-Jara, D. Moya-Loaiza, G. Abad-Farfán, A. Andrade-Galarza, Surgical planning and finite element analysis for the neurocraneal protection in cranioplasty with PMMA: A case study, Nati. Lib. Medicine, 8 (2022) e10706. https://doi.org/10.1016/j.heliyon.2022.e10706

[32] F. Moncayo-Matute, E. Vázquez-Silva, P. Torres-Jara, P. Peña-Tapia, D. Moya-Loayza, G. Abad-Farán, Mechanical analysis for personalized implant for neurocranial protection manufactured with Polymethylmethacrylate, J. Phys. Conf. Ser., 2516 (2023) 012005. https://doi.org/10.1088/1742-6596/2516/1/012005